Avalanches, transport, and local equilibrium in self-organized criticality

Afshin Montakhab and J. M. Carlson
Department of Physics, University of California, Santa Barbara, California 93106-9530
(Received 19 September 1997; revised manuscript received 7 August 1998)

We obtain numerical evidence of local equilibrium in a family of sandpile models which exhibit self-organized criticality (SOC), by comparing them with closed systems which exhibit dynamical depinning transitions. In particular, we construct a mapping between the open and closed system avalanche size distributions which accounts for finite size fluctuations in the density and the critical point. Our results suggest a generalization of the singular diffusion description of SOC which transcends the point where this description was previously seen to break down. [S1063-651X(98)15811-7]

PACS number(s): 64.60.Ht, 02.50.−r, 05.40.+j, 05.60.+w

I. INTRODUCTION

Local equilibrium is a useful property which leads to predictions for the nonequilibrium dynamics of open driven systems based on known aspects of their closed equilibrium analogs [1,2]. A driven system exhibits local equilibrium when its local properties are indistinguishable from those of an equilibrium system at the same density, in spite of the fact that the global behaviors may be quite different. It is not particularly unusual to find that local equilibrium applies in systems which exhibit a simple uniform flow. However, it is surprising to find equilibrium analogs for systems which exhibits large scale emergent phenomena.

Certain driven threshold systems have proven to be successful testbeds for applying local equilibrium in cases which exhibit complex phenomena over a broad range of scales [3–9]. In particular, analogies between self-organized criticality (SOC) [10] and the more traditional criticality which underlies dynamical phase transitions [11,12] have shown that local equilibrium can apply to systems in the neighborhood of a critical point. This analogy underlies the singular diffusion description of transport in certain SOC systems introduced by Carlson and co-workers [13–17]. In this analysis, SOC models are studied first as *closed* systems, for which there is a well-defined conserved quantity. In the hydrodynamic limit these systems are shown to satisfy deterministic diffusion equations in which the diffusion coefficient depends on the local value of the conserved density, and diverges as the density approaches a critical point. The key success of the singular diffusion description is obtained by applying it to the *open* systems that exhibit SOC, where it is found that with appropriate boundary conditions the diffusion limit correctly predicts the rate at which the average density approaches the critical value as the system size diverges.

More recently, it was shown that the diffusion description can break down when the open system is driven sufficiently hard [18]. In this scenario, as the driving rate is increased, fluctuations cause the density of a macroscopic portion of the system to exceed the critical value. This *a priori* rules out the possibility of applying the closed system thermodynamic singular diffusion limit to the open finite system, since the diffusion coefficient in this limit is undefined for densities greater than the critical density. Is this breakdown an indication that the open system no longer behaves similarly to the closed system?

In this paper we present evidence that the analogy between closed and open systems can survive beyond the point where the diffusion limit has failed. Thus, in the systems we consider, local equilibrium is found to be extremely robust as it survives in spite of systemwide fluctuations in the neighborhood of a thermodynamic singularity. Based on results we obtain for avalanche distributions in the closed and open systems, we suggest an extended relationship between relaxation on the closed system and transport on the open system. The key point is to compare the open driven system to an appropriate ensemble of closed systems of the same finite size which lie below their sample dependent depinning densities, and are distributed in density according to the fluctuations of the open driven system. The singularities associated with the critical density arise in the thermodynamic limit and are avoided by focusing on a selected subset of finite systems.

The remainder of this paper is organized as follows. In Sec. II we describe the open and closed systems that we have studied. In Sec. III we provide a brief review of depinning transitions and singular diffusions, highlighting the features which are particularly relevant for finite systems. In Sec. IV we define a necessary test for local equilibrium in terms of a mapping between event size distributions on the open system and the corresponding distributions on the closed system, and verify the mapping numerically in regimes where the singular diffusion limit holds and fails. In Sec. V we discuss the implications of local equilibrium for a more general relationship between relaxation on the closed system and transport on the open system which extends past the point where the deterministic diffusion limit fails. In Sec. VI we conclude by discussing why we expect local equilibrium is so robust in the class of models we have considered.

II. DEFINITION OF THE MODELS

All of the models we consider can be thought of as variations of the Bak, Tang, and Wiesenfeld (BTW) sandpile model [10], in which there is a ''mass'' m_i associated with each site on a two-dimensional $N\times N$ integer lattice. All the models share the same toppling rule, and differ only in the

boundary conditions and the manner in which avalanches are initiated.

A. Toppling rule

The site i ''topples'' when m_i exceeds a specified threshold value m_c. As a result m_i is reduced by a fixed amount which is subsequently redistributed among nearest neighbor sites $m_{\rm nn}$. Without loss of generality we take $m_c=4$, and the following toppling rule. If

$$m_i > m_c$$

then

$$m_i \rightarrow m_i - 4, \quad m_{\rm nn} \rightarrow m_{\rm nn} + 1. \tag{1}$$

The process in Eq. (1) is iterated for each of the $m_{\rm nn}$ that may have become unstable, until all of the sites on the lattice are below threshold. The cumulative result of an initial instability is referred to as an avalanche, and the avalanche size is the number of sites that topple.

B. Boundary conditions: open vs closed systems

Sandpile models are typically defined with open boundary conditions. The SOC steady state is reached when, on average, addition of mass balances loss of mass at the boundary. However, it is also possible to define closed versions of these systems in which the boundary conditions are periodic. In this case, when edge sites topple, one or more grains are transferred to an edge on the opposite side of the system. For a closed system, the toppling rule preserves the density, and there is a critical density at which the system exhibits a thermodynamically sharp phase transition between pinned and sliding states. As several authors have previously noted [12,19], there is a direct analogy between the closed system and a space-time discretization of the Fukyama-Lee-Rice model [20] for charge density waves (CDW's).

C. Driving mechanisms

We consider three driving mechanisms (equivalently, avalanche initiation rules). We refer to the first two as stirring mechanisms, because locally they rearrange the grains but do not result in a net change in the mass. In contrast, the third mechanism results in a net addition. The critical exponents characterizing the avalanche distributions are different in each case. This leads to different exponents characterizing the singular diffusion coefficient. See Table I.

1. Thermal driving

The thermal driving mechanism was introduced by Myers and Sethna [21] in the context of CDW's, and corresponds to initiating avalanches by randomly toppling subthreshold sites. That is, a site i on the lattice is chosen at random and is made to topple according to the usual toppling rule even though it is initially below threshold:

$$\begin{aligned} m_i &\rightarrow m_i - 4, \\ m_{\rm nn} &\rightarrow m_{\rm nn} + 1. \end{aligned} \tag{2}$$

TABLE I. Closed systems: The thermal, exchange, and ramping mechanisms described in Sec. II lead to different correlation length exponents [Eq. (9)], and different diffusion singularities [Eq. (8)], as reported in Refs. [12,18,21] and Sec. V.

Driving mechanism	Initiation rule	Correlation exponent	Diffusion singularity
Thermal	$m_i \rightarrow m_i - 4$ $m_{nn} \rightarrow m_{nn} + 1$	$\nu = 0.5$	$\phi = 1.7$
Exchange	$m_i \rightarrow m_i - 1$ $m_j \rightarrow m_j + 1$	$\nu = 0.75$	$\phi = 2.3$
Ramping	$m_i \rightarrow m_i + 1$	$\nu = 1$	

If any of the neighboring sites is above threshold, the toppling rule Eq. (1) is iterated until all sites are stable at which point another thermal kick [Eq. (2)] takes place.

2. Exchange driving

The exchange driving mechanism was introduced by Carlson *et al.* [18] in the context of SOC systems, and numerical results were obtained both on open and closed systems. Exchange driving corresponds to selecting a site i at random, removing one grain from that site, and depositing the grain on a randomly selected nearest neighbor of i:

$$\left.\begin{aligned} m_i &\rightarrow m_i - 1 \\ m_j &\rightarrow m_j + 1 \end{aligned}\right\} \quad \text{for a random neighbor } j \text{ of } i. \tag{3}$$

If m_j is above threshold, the toppling rule [Eq. (1)] is iterated until all sites are below threshold.

3. Ramping

Ramping is the most commonly considered driving mechanism for both CDW's and SOC. The original BTW sandpile model is driven this way by adding one grain at a time to a randomly chosen site i:

$$m_i \rightarrow m_i + 1. \tag{4}$$

If that site is above threshold, the toppling rule [Eq. (1)] is iterated until the system is completely stable. Of the three driving mechanisms, ramping is the only case in which mass is added to the system.

4. Mixed cases

To obtain nontrivial results for thermal or exchange driving of open systems we must include some probability of addition (i.e., ramping) to provide a net flux. We define the exponent d_A (for dimension of addition) so that on each initiation step of the automaton the ramping rule is invoked with probability

$$P_{\rm add} = N^{d_A}/N^d, \tag{5}$$

while a stirring event (either thermal or exchange toppling) takes place with probability

$$P_{\rm stir} = 1 - (N^{d_A}/N^d). \tag{6}$$

Therefore, $d_A = d = 2$ corresponds to pure ramping. Furthermore, by varying d_A we vary the flux, and it has been shown previously that when d_A is sufficiently large the singular diffusion description breaks down [18].

III. DIFFUSION LIMITS, DEPINNING TRANSITIONS, AND LOCAL EQUILIBRIUM

Local equilibrium implies the existence of a relationship between relaxation on the closed system and transport on the open system. In this section we highlight several established features associated with transport and relaxation in the models defined in Sec. II. Typically, both relaxation and transport are analyzed in the continuum limit in terms of deterministic quantities—relaxation rates or diffusion coefficients. However, the continuum limits are subtle in the models we consider because both relaxation and transport take place in the neighborhood of a critical point. Here we give special attention to finite size effects. Accounting properly for the finite system size is at the heart of the mapping we construct in Sec. IV.

Previous work by Carlson *et al.* [13] exploited the analogy between relaxation and transport in the development of the singular diffusion description of SOC systems. They studied the continuum limits of a class of sandpile models which were found to satisfy deterministic singular diffusion equations. These equations describe the evolution of a conserved density ρ, which is the continuum version of the discrete mass variable m_i. As $N \to \infty$, the automata map onto deterministic diffusion equations which describe the net effect of many (infinite in the limit) avalanches, involving many particles and many sites.

The singular diffusion equations are of the general form:

$$\frac{\partial \rho}{\partial t} = \nabla \cdot [D(\rho) \nabla \rho], \tag{7}$$

where the diffusion coefficient depends on the local density and exhibits a singularity at a critical density ρ_c,

$$D(\rho) \sim \frac{1}{(\rho_c - \rho)^{\phi}}. \tag{8}$$

In the closed system the critical density is associated with a depinning transition which has been studied in the context of CDW's [11,12,22,23]. When the system is prepared with density $\rho \geq \rho_c$ in the thermodynamic limit with probability 1, there will be an infinite avalanche which propagates forever.

The diffusion coefficient is only defined for $\rho < \rho_c$ (the microscopic time scale which enters into the continuum limit is the avalanche initiation rate, while in the depinned state this time scale is undefined since an infinite avalanche begins in the initial state and never stops). A diverging diffusion coefficient reflects the fact that typical transition lengths (event sizes) are diverging as the density approaches the critical value ρ_c. Indeed, numerical studies of event size distributions on closed systems [12,18,21,24] reveal a characteristic length scale which diverges at the transition

$$\xi(\rho) \sim \frac{1}{(\rho_c - \rho)^{\nu}}. \tag{9}$$

Here $\xi(\rho)$ measures how far an instability will typically propagate before the system relaxes to a metastable state.

The singular diffusion coefficient can be evaluated numerically on the closed system at fixed density $\rho < \rho_c$ by monitoring the relaxation of a nonequilibrium density profile to the uniform equilibrium state (see Sec. V). However, the key success of this description comes from *assuming* that the same equation describes transport on the open system subject to the boundary conditions associated with the external driving mechanism and the dissipation. For SOC systems the finite system size always remains relevant, and arises in conjunction with Eq. (7) via the rescaled addition rate [Eq. (5)], which is seen to increase with system size [13]. Ultimately this leads to the prediction that the steady state density approaches the singularity as the system size diverges.

The rate of convergence is obtained self consistently by assuming the average density $\overline{\rho}$ is of the form

$$\rho_c - \overline{\rho} \sim \frac{1}{N^b}. \tag{10}$$

The exponent b is determined by balancing the time scale associated with addition,

$$\tau_A \sim \frac{1}{N^{d_A} N^{b-d}}, \tag{11}$$

with that for diffusive transport,

$$\tau_D \sim N^{2-b\phi}. \tag{12}$$

Here τ_A is the inverse rate at which the mass is increased by an amount comparable to the distance from the singularity, and τ_D is the inverse relaxation rate of a density perturbation in Eq. (7), obtained by reintroducing the explicit system size dependence of the spatial and temporal variables. A steady state is obtained for the density at which these time scales are equal, yielding the exponent

$$b = \frac{2 - d + d_A}{\phi - 1} \tag{13}$$

as the self-consistent solution in Eq. (10). This implies that the rate of convergence to the critical density with system size N increases as the addition rate exponent d_A is increased.

Because the density approaches a singularity as $N \to \infty$, application of the continuum description in Eq. (7) to an open driven system can fail. In previous work on applying singular diffusions to SOC models, the breakdown of the diffusion limit was identified with a particular value of the driving rate exponent d_A [Eqs. (5) and (6)] at which fluctuations associated with the finite size of the open system leads the density to exceed the critical density in macroscopic domains.

We characterize fluctuations in the open system density distribution by the exponent a, such that

$$\sigma \equiv [\langle \rho^2 \rangle - \langle \rho \rangle^2]^{1/2} \sim N^{-a}. \quad (14)$$

In the case of the BTW model, the fluctuations obey the central limit theorem (consistent with the fact that the mass-mass correlation length does not diverge at ρ_c in this system), so that $a = d/2$. Density fluctuations exceed the critical point when $a \leqslant b$, so that the thermodynamic diffusion limit is no longer self-consistent in that regime.

In this paper we extend the analogy between open and closed systems by comparing the open system to a finite closed system of the same size, rather than using results obtained for a continuum limit on the closed system as was done before. The key point is to account for both the density fluctuations of the finite open system and the critical point fluctuations of the ensemble of finite closed systems [12,24]. If both kinds of fluctuations are small compared to the distance between the mean open system density and the thermodynamic singularity, then predictions based on singular diffusion in the $N \to \infty$ limit survive. In this case, it is always possible to find a finite system which is large enough that the effects due to fluctuations can be made smaller than a specified tolerance.

Alternately, to describe systems which approach the critical density faster than the fluctuations decay, it is necessary to account for the possibility of overlap between density fluctuations on the open system (characterized by the exponent a as described above) and the critical point fluctuations of the ensemble of closed systems. An ensemble of closed systems (involving different realizations of the randomness), is characterized by a distribution of critical densities ρ_c^s. The width of this distribution is characterized by a finite size scaling exponent [25]

$$\sigma' \equiv [\langle (\rho_c^s)^2 \rangle - \langle \rho_c^s \rangle^2]^{1/2} \sim N^{-1/\nu_{\mathrm{FS}}}. \quad (15)$$

In the systems we consider these fluctuations obey the central limit theorem $\nu_{\mathrm{FS}} = d/2$ [11]. This is the same scaling as that obtained for the open system density fluctuations, i.e., $1/\nu_{\mathrm{FS}} = a$, so that as the system size diverges ($N \to \infty$), the fluctuations in both the open system density and closed system critical point converge to zero at the same rate, which preserves the criterion $b < a$ for which fluctuations are irrelevant and the thermodynamic singular diffusion limit applies to the open system. In contrast, for $b \geqslant a$ fluctuations become dominant.

The two different scenarios are illustrated in Fig. 1, where we plot various distributions for a 64×64 exchange model. The curve on the right side of each part (a) and (b) is the critical point distribution on the closed system, $F_c^N(\rho_c^s)$. This is measured by ramping from the same set of initial conditions (e.g., $m_i = 0, \forall i$) and recording the value of the density at which an infinite avalanche (i.e., a sliding state) occurs. On the left side of Fig. 1(a) we plot the middle quarter open system density distribution $G_o^N(\rho)$ for $d_A = 1.0$ with exchange stirring. Results based on density estimates made from the middle quarter of the system sometimes yield better results than those obtained using the density averaged over the full system, because restricting measurements to the middle quarter avoids edge effects. In this regime $b < a$, so that fluctuations decay more rapidly than the density converges to the critical point, and thus the singular diffusion description applies. In Fig. 1(b), we plot the density for both the middle quarter of the system as well as the full system for the BTW model with $d_A = 2.0$. In this regime $b > a = 1/\nu_{\mathrm{FS}}$, and the distributions already overlap for $N = 64$, signaling the breakdown of the deterministic diffusion limit. The middle quarter density distribution overlaps more strongly with the distribution of critical points than the corresponding distribution for the whole system. This occurs because the mean of the middle quarter distribution is slightly higher (it does not include the low density boundary layers), and the middle quarter corresponds to a smaller subsystem with an intrinsically greater variance [26].

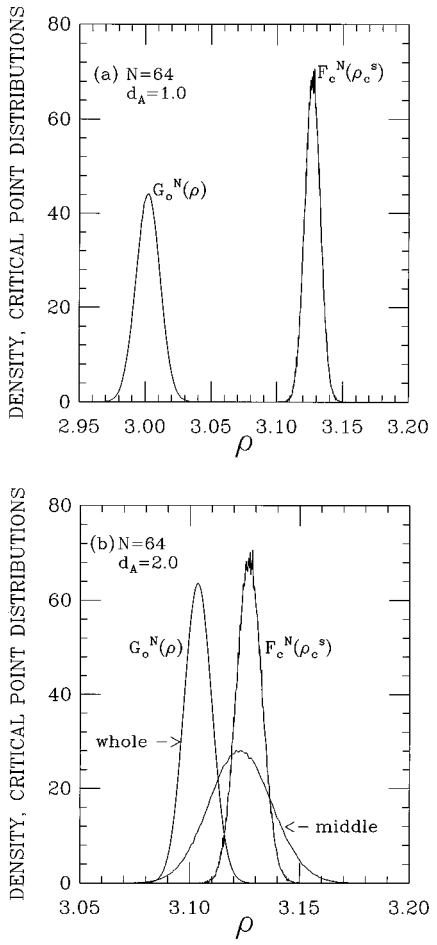

FIG. 1. Distributions of the open system densities $G_o^N(\rho)$, and closed system depinning threshold densities $F_c^N(\rho_c^s)$, for a 64×64 exchange model. In (a), $d_A = 1.0$, and fluctuations are small compared to the separation between the mean density and the mean depinning threshold. In this case we have plotted the middle quarter density distribution. In (b), $d_A = 2.0$, and the mean density is much closer to the mean depinning threshold so that the distributions overlap. Both middle quarter and full system densities distributions are included for comparison.

IV. AVALANCHE DISTRIBUTIONS

In this section we propose a mapping between the open and closed systems which extends beyond the point where fluctuations destroy the deterministic diffusion limit. We discuss our map in the context of the avalanche distributions.

However, the analogy we make is easily generalized and has also been tested for other quantities [27]. The mapping is a necessary, but not sufficient, condition to verify local equilibrium. A more stringent test would involve a detailed check of all correlation functions. However, we are ultimately most interested in whether the aggregate transport on the open system has an analogy in closed system dynamics, rather than in details of the microscopic states. A check of the mapping between avalanche distributions provides fairly convincing evidence that the transport properties will be similar.

A. Open system compared to an ensemble of closed systems

A specific scaling form of the avalanche distribution on the closed system has been conjectured and verified numerically in previous studies [12,18,24]. Near the critical point we write

$$P_c^N(n,\rho) \sim \frac{1}{n^\alpha}\, g(n/\xi^d), \tag{16}$$

where $P_c^N(n,\rho)$ is the equilibrium probability of an event involving n sites at density ρ on a system of size N, and $g(x)$ is a scaling function. The subscript ''c'' denotes a closed system. This relation defines the exponent α. The correlation length is given by Eq. (9), and provides the (typically exponential) cutoff in the event size distribution.

The steady state density of the open system exhibits central limit fluctuations about a mean density $\overline{\rho}$, which also scales with N. We write the probability of the open system having a density ρ as

$$G_o^N(\rho) = \frac{1}{\sqrt{2\pi}\sigma} \exp[-(\rho-\overline{\rho})^2/2\sigma^2]. \tag{17}$$

Here the subscript ''o'' denotes open system and the superscript N reminds us of the implicit system size dependence of the mean $\overline{\rho}$ and the variance σ. A similar expression characterizes the Gaussian distribution of critical densities ρ_c^s on the finite closed system

$$F_c^N(\rho_c^s) = \frac{1}{\sqrt{2\pi}\sigma'} \exp[-(\rho_c^s-\rho_c)^2/2\sigma'^2], \tag{18}$$

where $\sigma' \sim N^{-1/\nu_{\rm FS}}$ with $\nu_{\rm FS} \geqslant 2/d$.

We now construct the mapping for the event size distribution on the open system $P_o^N(n)$ in terms of $P_c^N(\rho,n)$. The key point is to consider the open system as an ensemble of closed systems which are weighted according to their densities and their finite size, and restricted to be the subset of systems below their sample dependent critical points. To this end, we integrate the closed system event size distribution $P_c^N(\rho_n)$ over the distribution of densities of the open system $G_o^N(\rho)$, and perform an ensemble average by integrating over the distribution of threshold densities $F_c^N(\rho_c^s)$ for closed systems of the same finite size:

$$P_o^N(n) \sim \int_{-\infty}^{+\infty} \int_{-\infty}^{\rho_c^s} P_c^N(n,\rho) \left[\frac{G_o^N(\rho) F_c^N(\rho_c^s)}{I} \right] d\rho\, d\rho_c^s. \tag{19}$$

The left hand side is simply the open system event size distribution, while the right hand side represents the distribution we construct from an ensemble of closed systems. The inner integral performs an average over the (spatially varying) density of the open system for densities below the critical point and the outer integral averages over the fluctuating critical point. Here I is defined by $I = \int_{-\infty}^{\rho_c^s} G_o^N(\rho')d\rho'$, which normalizes the open system density distribution subject to the restriction $\rho < \rho_c^s$. This normalization factor is needed since the two probability functions may overlap significantly. We integrate the density ρ only up to the cutoff ρ_c^s, because the open boundary conditions prevent infinite events from occurring on the open system. Thus they must be excluded from the closed system ensemble. Finally, we note that this map does not require the distributions to be of the specific forms given in Eqs. (16)–(18), and is easily generalized to other measurable quantities by substituting the distributions of interest for $P_c^N(\rho,n)$ and $P_o^N(\rho)$ in Eq. (19).

Finally, we consider Eq. (19) in the $N \to \infty$ limit for the specific distributions given in Eqs. (16)–(18). While Eq. (19) does not depend on the diffusion limit, there are two different regimes which coincide with the conditions for which the limit holds and fails. In the simplest case the density fluctuations do not overlap the critical point fluctuations. Therefore, without loss of generality, we replace ρ_c^s by ∞ in the upper limit of the integration so that as N diverges, the Gaussians converge to δ functions, resulting in the prediction

$$P_o^N(n) \sim \frac{1}{n^\alpha}\, g(n/\xi^d) \quad (a > b), \tag{20}$$

where $\xi \sim (\rho_c - \overline{\rho})^{-\nu}$. Note that the predicted open system event size distribution has an implicit system size dependence since $\overline{\rho}$ scales with N according to Eq. (10). This describes the case when diffusion holds, and our mapping simply states that the event size distributions of the open and closed systems should have the same form having identical exponents ν and α. On the other hand, when there is an overlap between the open system density fluctuations and closed system critical point fluctuations, the hydrodynamic singular diffusion limit breaks down. Nonetheless, we can carry out the integrals by elementary methods to obtain

$$P_o^N(n) \sim \frac{1}{n^\alpha} \quad (a < b). \tag{21}$$

In this case the maximum event saturates at the system size, and the predicted power law is only limited by the finite size of the system. The exponent α is again expected to be the same on the open and closed systems.

B. Numerical results

We numerically verify Eq. (19), in which the open SOC system is compared to an ensemble of closed finite systems

TABLE II. Open vs closed: The table summarizes the results obtained from finite size scaling collapses in Figs. 2–5. In each case, the avalanche distributions obtained for the open driven system collapse with the same exponents, like those used for the ensemble of closed finite systems defined according to the mapping in Eq. (19). Thus the analogy between closed and open systems persists in the soft ($d_A=1.0$), intermediate ($d_A=1.5$), and hard ($d_A=2.0$) driving regimes.

Driving mechanism	Open system driving rate	Avalanche exponent	Correlation exponent	Diffusion applies	Open/closed exponents agree
Thermal	$d_A=1.5$	$\alpha=1.16$	$\nu=0.49$	no (as $N\to\infty$)	yes
Exchange	$d_A=1$	$\alpha=1.41$	$\nu=0.76$	yes	yes
Exchange	$d_A=1.5$	$\alpha=1.28$	$\nu=0.79$	no (as $N\to\infty$)	yes
Ramping	$d_A=2$	$\alpha=1.18$	saturates	no	yes

for the class of BTW sandpile models introduced in Sec. II. We consider the open system as a function of driving rate d_A and system size N. In each case we initiate many avalanches in the statistically stationary state to determine the avalanche distribution function $P_o^N(n)$ and the density distribution function $G_o^N(\rho)$. Then for each closed system of size N we begin with $\rho=\rho_{\min}=0$, and add one grain at a time. After the grain is added, the system is stirred at fixed density for a long time as we accumulate statistics for $P_c^N(\rho,n)$. After a large number of events have taken place another grain is added, and contributions to $P_c^N(\rho,n)$ for the next density increment are obtained. If at any point an infinite avalanche is encountered, the data for that specific density are discarded and the density is reset to $\rho_{\min}$ for another sweep. In this manner we approximate the process of integrating densities up to the critical density ρ_c^s. Finally, we combine the closed system events distributions obtained for different densities and weight them according to the observed open system distribution of densities $G_o^N(\rho)$ to obtain an estimate for the right hand side of Eq. (19).

We compare the distribution constructed from the ensemble of closed systems with the open system events distribution in terms of the scaling exponents extracted from a finite size scaling collapse. Since the event size n is rescaled by the characteristic size $\xi^d\sim(\rho_c-\overline{\rho})^{-\nu d}\sim N^{b\nu d}$, we may replace Eq. (20) with $P_o^N(n)\sim(1/n^\alpha)g(n/N^{b\nu d})$. Then defining $z\equiv n/N^{b\nu d}$, the expected scaling takes the form

$$P_o^N(n)N^{\alpha b\nu d}\sim\frac{1}{z^\alpha}\,\hat{g}(z). \tag{22}$$

For a given driving rate (d_A) and a stirring mechanism (thermal or exchange), we obtain the distributions for different system sizes and perform a finite size collapse. The best fit x-axis scaling exponent gives an estimate of $b\nu d$, and the best fit y-axis exponent gives an estimate for $\alpha b\nu d$. The ratio of the two exponents yields α, and ν can be calculated given the estimate of b which can be obtained by computing the mean values of the density distributions $G_o^N(\rho)$ as a function of N.

We consider three different regimes. *Soft driving* describes the case in which $a>b$, and the deterministic singular diffusion applies as $N\to\infty$. *Intermediate driving* describes the case in which b is larger but comparable to a, and the deterministic diffusion limit is expected to be invalid in the $N\to\infty$ limit. We introduce this as a separate case from the hard driving regime discussed below, because we find that in the marginal case for the system sizes we can consider, the distributions do not overlap, and many of our numerical results are still consistent with the singular diffusion limit. Finally, we consider *hard driving*, which is exhibited by the standard BTW model with pure ramping. In this regime $b>a$, and a significant overlap of density and critical point fluctuations occurs even for small systems so that a pure power law in the event size distribution is observed. The results are presented in summary form in Table II.

1. Soft driving: $d_A=1.0$

We first consider the open exchange model with $d_A=1.0$, where fluctuations are small compared to the distance from the singularity. A finite size scaling collapse of the avalanche size distributions is shown in Fig. 2(a) for $N=16$, 32, 64, and 128. We compare this collapse with the one obtained from closed systems of the same sizes, where each closed system distribution is constructed according to Eq. (19) from an ensemble of closed exchange models weighted by the distribution of densities obtained for the middle quarter of the open system. Middle quarter densities are chosen in order to avoid the edge effects associated with boundary layers, as discussed in Ref. [13]. The result for the ensemble of closed systems is shown in Fig. 2(b), where an excellent collapse is obtained for the same set of exponents as in Fig. 2(a), indicating that the mapping between the open and closed systems applies.

The ratio of the exponents yielding the best collapse produce the estimate $\alpha=1.41$. Computing b from our numerical data on middle quarter densities yields $b=0.73$ [in reasonably good agreement with the value predicted by singular diffusions in Eq. (13)], and from this we obtain $\nu=0.76$ which compares well with the value of ν obtained previously for the closed system in Ref. [18].

2. Intermediate driving: $d_A=1.5$

Next we consider the open exchange model with $d_A=1.5$. In Fig. 3(a) we show a finite size scaling collapse of the open system avalanche distributions for system sizes up to 512×512. Figure 3(b) illustrates that the analogous closed system results [based again on Eq. (19), with the middle quarter density distribution from the open system] collapse well with the same exponents. In this case, we have included only the largest system sizes, $N=128$, 256, and 512, because the smaller system sizes deviated from this collapse systematically with decreasing size. From this we obtain $\alpha=1.28$. Computing the value of b from the open system densities we

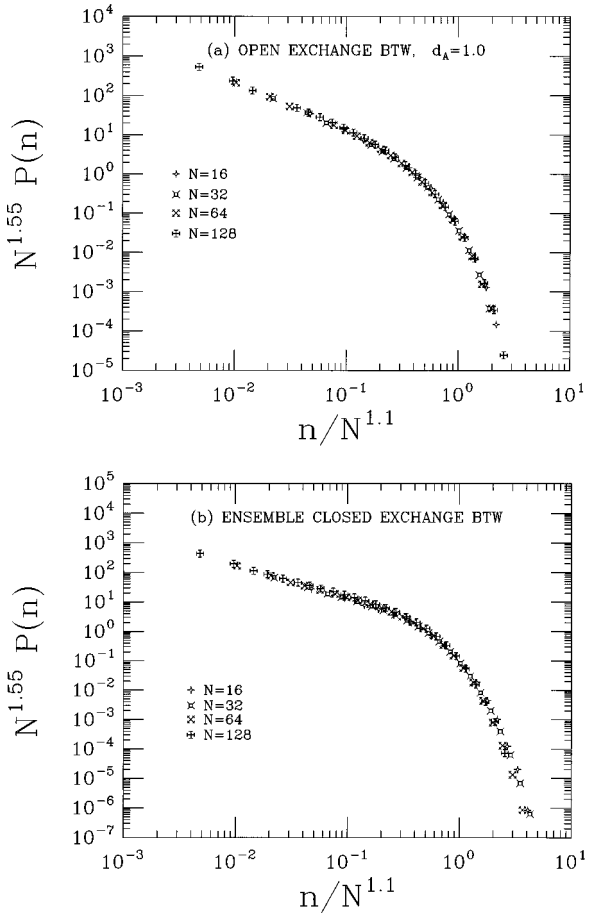

FIG. 2. Finite size scaling collapse of the avalanche distributions for exchange stirring with $d_A=1.0$. The same scaling exponents give a good collapse for both (a) the open system and (b) the ensemble of closed systems. From this fit we obtain $\alpha=1.41$ and $\nu=0.76$.

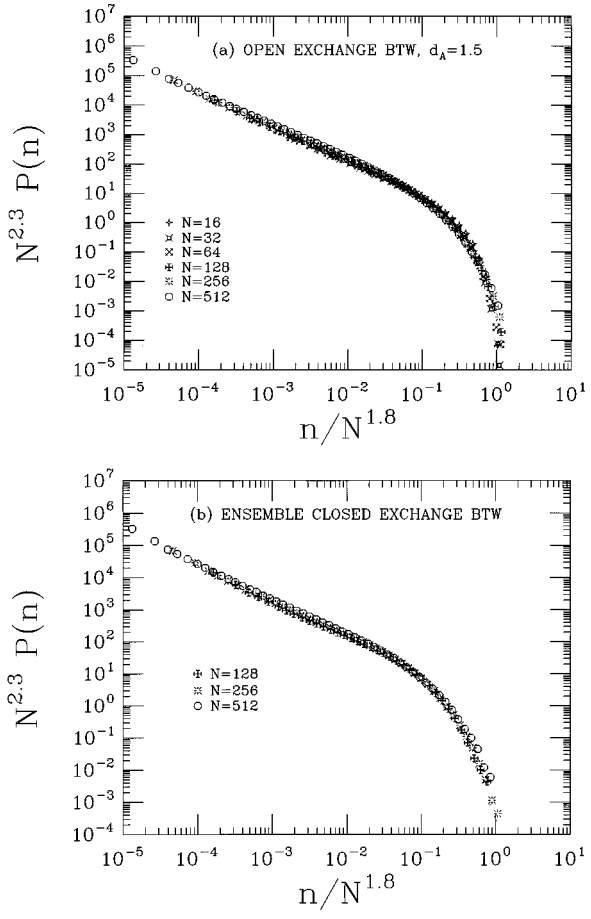

FIG. 3. Finite size scaling collapse of the avalanche distributions for exchange stirring with $d_A=1.5$. The same scaling exponents give a good collapse for both (a) the open system and (b) the ensemble of closed systems. From this fit we obtain $\alpha=1.28$ and $\nu=0.79$.

obtain $b=1.135$, in good agreement with Eq. (13). This yields $\nu=0.79$, which is again consistent with the closed system results.

We have also considered thermal stirring in the intermediate regime. Figure 4(a) illustrates the finite size scaling collapse of avalanche distributions on the open thermal system with $d_A=1.5$ and $N=16$, 32, 64, 128, 256, and 512. In Fig. 4(b) we show that the exponents used for the collapse also collapse the data obtained from the closed system ensembles. In this case we obtain $\alpha=1.16$. The open system middle quarter mean densities yield the estimate $b=1.57$, which in turn gives $\nu=0.49$, which is consistent with value of $\nu=0.5$ previously obtained on the closed system [21].

Thus we have established a correspondence between the open and closed systems for $d_A=1.5$, and obtained correlation length exponents ν which are consistent with previous studies on the closed systems. However, there remains a subtle discrepancy between the data we have obtained, and the predictions we have made based on the dominance of fluctuations that we anticipate for large enough N with this value of d_A. Since $\phi=2.3$ for exchange stirring [18], fluctuations should dominate when $d_A \geqslant 1.3$. We have found $\phi=1.7$ for thermal stirring (see Sec. V), so fluctuations should dominate when $d_A \geqslant 0.7$ in that case. However, the distributions $G_o^N(\rho)$ and $F_c^N(\rho_c^s)$ do not overlap for the system sizes we can consider.

As shown earlier, the failure of the diffusion limit coincides with the emergence of pure power laws in the events distribution [Eq. (21)]. In other words, we expect that $\xi \sim N$, i.e., the characteristic length scale should exhibit a finite size crossover and saturate at the system size. In general the correlation length has a finite size scaling form

$$\xi \sim \frac{1}{(\rho_c-\rho)^{\nu}} H(N(\rho_c-\rho)^{\nu}). \tag{23}$$

The scaling function $H(z)$ approaches a constant for $z \gg 1$, since in the thermodynamic limit the correlation length is independent of the system size. Alternately, $H(z) \sim z$ for $z \leqslant 1$ so that when $(\rho_c-\rho)^{-\nu} \approx N$ the correlation length becomes finite size limited, $\xi \sim N$. One cannot expect to extract the exponent ν in this regime. As we shall see, this saturation is observed when $d_A=2.0$. However, when $d_A=1.5$, even though the singular diffusion limit is asymptotically expected to fail, for the finite systems considered the correlation length has not saturated. Instead, our data collapse indicates that over this range of system sizes the characteristic lengths are decreasing slightly relative to the system size: $\xi \sim N^{0.9}$ for

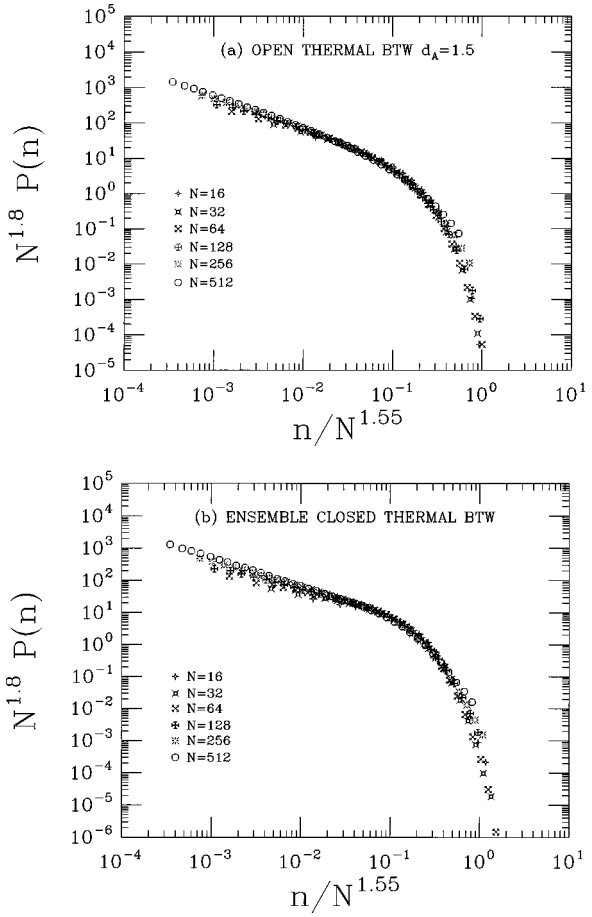

FIG. 4. Finite size scaling collapse of the avalanche distributions for thermal stirring with $d_A=1.5$. The same scaling exponents give a good collapse for both (a) the open system and (b) the ensemble of closed systems. From this fit we obtain $\alpha=1.16$ and $\nu=0.49$.

exchange stirring in Fig. 3, and $\xi\sim N^{0.78}$ for thermal stirring in Fig. 4 (the exponent describing the scaling of ξ with N is obtained by dividing the exponent for the x-axis data collapse by $d=2$). We expect that this discrepancy results from the fact that we are not yet in the asymptotic regime for this driving rate. Extrapolations of higher order fits of the numerical results suggest that very large system sizes would be required to achieve the predicted asymptotic results [18]. This discrepancy does not invalidate our test for local equilibrium. While the values of ν obtained from these fits are consistent with closed system results, we suspect they may not represent asymptotic results.

3. Hard driving: $d_A=2.0$

Finally we consider $d_A=2.0$, where the system sustains the maximum flux. The exchange and thermal models are indistinguishable in this case. In Fig. 5(a) we plot a finite size scaling collapse of the open system avalanche distributions which are described by pure power laws with sharp cutoffs at the system size. The x-axis scaling exponent is $d=2.0$, indicating that $\xi\sim N$, as expected in this regime.

We construct the analogous distribution for the ensemble of closed systems initiating avalanches by ramping only. The result of a finite size scaling collapse in this case is shown in

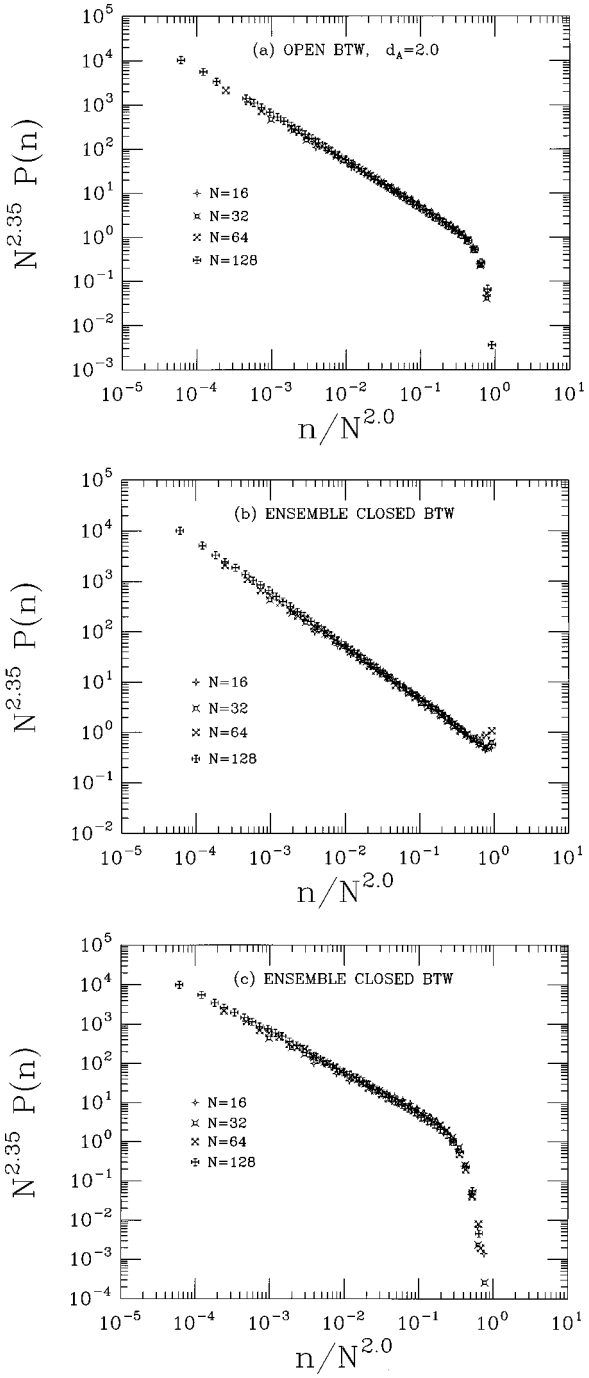

FIG. 5. Finite size scaling collapse of avalanche distributions for the standard BTW model, i.e., $d_A=2.0$. The same exponents give a good collapse for (a) the open system, (b) the ensemble of closed systems weighted according to the middle quarter density distribution, and (c) the ensemble of closed systems weighted according to the full system density distribution. We obtain $\alpha=1.175$ from this fit, and the saturation value $\xi\sim N$ associated with a power law distribution.

Fig. 5(b) for the density distribution obtained from the middle quarter of the open system. While the data do collapse with the same exponents here as in Fig. 5(a), we obtain better agreement for the scaling function when the integral in Eq. (19) is based on the full system density, as shown in Fig. 5(c). The primary difference is in the tail of the distribution. The distribution constructed using the middle quarter densi-

ties exhibits excess large events which we do not observe on the open system. This occurs because the mean of the middle quarter density distribution is essentially pinned at ρ_c even for relatively small systems. In addition, the middle quarter density distribution is based on a smaller subsystem size than the distribution obtained numerically for the closed $N\times N$ system, so the variance is larger, which adds more weight to the tail. For these reasons, in spite of the inclusion of the boundary layers (which are less significant because they are sharper for hard driving), the full system density distribution gives a better fit.

Dividing the *y*-axis scaling exponent by the *x*-axis scaling exponent, we obtain the value of $\alpha=1.175$, which is consistent with that obtained from the CDW model by Narayan and Middleton [28]. We observe that $b=1.33$, obtained from whole system densities which combined with $d=2$, yields $\nu=0.75$, consistent with the value reported by Tang and Bak [23] for the same system, but inconsistent with the value $\nu=1.0$ reported by Narayan and Middleton for the closed system [12]. For the open system the characteristic length ξ saturates when the exponent for the *x*-axis data collapse is equal to 2.0, which is associated with the finite size limited case $\xi\approx N$. Therefore, this method of estimating ν breaks down on the open system.

V. CLOSED SYSTEM RELAXATION AND OPEN SYSTEM TRANSPORT

Given the fact that the analogy between event size distributions on the open and closed systems persists beyond the point where our previous hydrodynamic description fails, it is natural to ask whether a relationship between closed system relaxation and open system transport extends to this regime. The existence of a mapping between open and closed system event size distributions does not *a priori* imply that this will be the case, particularly since relaxation involves initializing the system in a nonequilibrium state.

Below, we suggest a generalization of the singular diffusion description which incorporates a finite size scaling crossover when the hydrodynamic limit breaks down. In this regime transport and relaxation are intrinsically noisy and finite size limited. Our results remain somewhat speculative due to computational limitations which prevent us from considering asymptotically large system sizes. Nonetheless we present numerical results for ensemble averages which are consistent with this picture.

The singular diffusion limit is described by Eq. (7), where the diffusion coefficient is given by Eq. (8). The specific scaling used to obtain a precise and deterministic continuum limit technically involves taking the system size to infinity on a closed system, as described in Sec. III. For any finite system the evolution is stochastic, to first approximation governed by a fluctuation equation described in Ref. [18] which represents the leading order finite size correction to the deterministic diffusion limit.

The subtlety comes in applying the diffusion limit to open systems, where it predicts that the density approaches the singularity as the system size diverges. When hydrodynamics holds, the fluctuations still decrease rapidly compared to the rate at which the density approaches the singularity, so that the system becomes more and more deterministic as $N\rightarrow\infty$. When diffusion fails, the fluctuations are of the same order as the gap between the density of the finite system and the singularity, so that the fluctuations remain significant for all system sizes. It is in this sense that the system is intrinsically noisy.

In order to motivate our description for the regime in which the hydrodynamic limit fails, it is useful to note that in some cases $D(\rho)$ has also been expressed in terms of the characteristic length scale $\xi(\rho)$ [Eq. (9)] associated with the cutoff in the event size distribution [29]:

$$D(\rho)\sim\frac{1}{(\rho_c-\rho)^{\phi}}\sim\frac{\xi^2}{\tau}. \tag{24}$$

When time is defined conventionally, e.g., if individual topplings occurred in a fixed, finite period of time, then we would expect the characteristic time scale τ to exhibit critical slowing down in the neighborhood of the ρ_c. However, in our case the clock is set by the stirring and/or addition rates rather than the local toppling rule, and individual events are viewed as instantaneous regardless of their size. Consequently, the time scale τ is associated with the rate of change of the pinned configurations, which will also depend on ρ, and is expected to *decrease* when approaching the singularity, since more sites change state as the typical avalanche size ξ increases. Borrowing the conventional notation from critical phenomena, we have

$$\tau\sim\xi^z \quad \text{with} \quad z<0, \tag{25}$$

so that

$$D(\rho)\sim\xi^{(2-z)}. \tag{26}$$

In Sec. IV we saw that the regime where diffusion fails is associated with a finite size scaling crossover as described by Eq. (23), such that for large enough densities on a given system size the largest events are limited not by the thermodynamic cutoff but rather by the system size $\xi\sim N$. The fact that the diffusion coefficient can be expressed in terms of ξ, and ξ exhibits finite size scaling, suggests a finite size scaling description of the diffusion coefficient:

$$D_N(\rho)\sim\frac{1}{(\rho_c-\rho)^{\phi}}\,K(N(\rho_c-\rho)^{\nu}). \tag{27}$$

When the system size is large compared to the event size cutoff, the argument x of the scaling function $K(x)$ is large. In this limit we expect $K(x)$ to approach a constant asymptotic value, so that the hydrodynamic result is retained. However, like ξ, the collective transport and relaxation dynamics which are characterized in terms of $D_N(\rho)$ are also expected to saturate at system size dependent average values when $x\leqslant 1$. Thus we expect $D_N(\rho)\sim N^{\theta}$, where scaling suggests $\theta=\phi/\nu=2-z$. In this case, $D_N(\rho)$ represents an ensemble average coefficient. For a specific realization transport and relaxation remain intrinsically noisy and the critical density ρ_c in Eq. (27) is sample dependent.

To verify this numerically, we apply the same algorithm used previously to determine the diffusion singularity, but

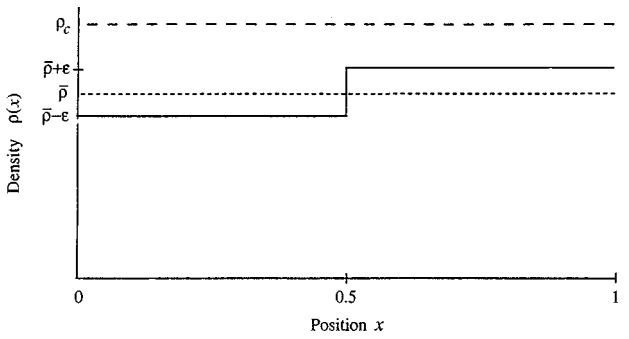

FIG. 6. Closed system relaxation rates are obtained numerically from an ensemble of systems for which the average initial state corresponds to a low amplitude step function in the density, as illustrated schematically here. In order to obtain the leading order linear results, the amplitude ϵ is taken to be small compared to the distance from the singularity $(\rho_c-\overline{\rho})$, and finite size effects become important when $\xi_N(\overline{\rho}-\epsilon)$ becomes comparable to N. The step function describes a cross section of the density variation along one axis of the two-dimensional lattice. The other direction is uniform.

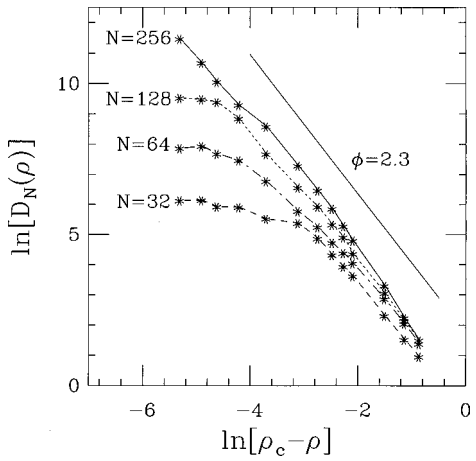

FIG. 7. Relaxation rate as a function of density and system size for closed finite systems with exchange driving. As ρ approaches $\rho_c \approx 3.125$, the rate is initially proportional to the singular diffusion coefficient [Eq. (8)] with $\phi \approx 2.3$. However, as the characteristic event size ξ becomes comparable to the system size, the relaxation rate saturates in a manner which scales with system size, consistent with Eq. (27).

extend our analysis to the regime where the system size becomes relevant. In particular, we monitor the time dependence of the relaxation of small amplitude perturbations. We consider an ensemble of closed systems initialized so that the average state is represented schematically by Fig. 6, which depicts the hydrodynamic density as a step function. Each element of the ensemble is prepared in a random initial state in which half of the system is at density $\overline{\rho}-\epsilon$, and the other half is at density $\overline{\rho}+\epsilon$. We then equilibrate each half separately at these offset densities, and combine the system and monitor the amplitude $A(t)$ of the offset for that sample as a function of time. Finally, we perform an ensemble average of $\langle A(t)\rangle$ to obtain the linear relaxation rate.

In the hydrodynamic case, the singular diffusion exponent ϕ can be determined using this method. When the initial offset is sufficiently small, we linearize Eq. (7) about the uniform density state $\rho(\mathbf{x})=\overline{\rho}$ to obtain

$$A(t) \approx A(0)\exp(-\lambda^2 D(\overline{\rho})t), \tag{28}$$

where λ is the eigenvalue of the (primary) Fourier mode which we monitor. In order for the hydrodynamic limit to apply, it is necessary for the largest events associated with the higher initial offset density to be small compared with half the total system size. To stay within this limit, yet get close enough to the singularity to see the asymptotic scaling of $D(\rho)$, is numerically time consuming. While in principal it should be possible to omit the ensemble average for the hydrodynamic case, in practice we cannot consider systems which are large enough to be self-averaging. Instead we average over many initial states, as described above. Using this method we have obtained the diffusion exponents $\phi=2.3$ for the exchange model and $\phi=1.7$ for the thermal model as reported in Table I.

To estimate the relaxation rate when the deterministic diffusion description fails, we extend our measurements on ensembles of closed, finite systems to higher densities, such that the largest events span an appreciable fraction of the system. In this regime, critical point fluctuations are also relevant, so ensemble averages are *a priori* necessary in order to identify the mean rate of decay. As for the closed system event size distributions, here we restrict the ensemble to the subset of systems which remain below their sample dependent critical points throughout the relaxation process.

The results are presented in Fig. 7 for the exchange model. Similar results were obtained for the thermal model. Our measurements were made for an initial density offset corresponding to 10% of the difference between the average density $\overline{\rho}$ and the singularity $\rho_c \approx 3.125$. We find that the decay remains roughly exponential, so that we can still estimate the ensemble average rate of decay using a least squares fit to the form given in Eq. (28). As illustrated, it exhibits a crossover at values of the density which increase with increasing system size, consistent with the finite size scaling form proposed in Eq. (27). For smaller densities the diffusion coefficient is (roughly) independent of system size and of the expected form [Eq. (8)]. However, as the density approaches the singularity, the relaxation rate saturates at values and densities which increase with system size.

The approximately equal spacing of the saturation value on the logarithmic scale for the three smaller system sizes is consistent with finite size limited form of $D(\rho)\sim N^{\theta}$, though with so few data points it would be unreasonable to evaluate θ numerically. At higher densities the events become increasingly large and time consuming, and an increasing number of realizations within the ensemble must be discarded because they exceed their (sample dependent) critical points. This prevents us from exploring densities which were sufficiently large to obtain saturation in the relaxation rate for larger systems.

What are the implications for transport on the open system? As discussed in Sec. III, when hydrodynamics holds the singular diffusion equation predicts the rate at which the density approaches the singular point as the system size diverges according to Eq. (10), where the exponent b in Eq. (13) is obtained by balancing the time scale τ_A associated with the addition of new particles [Eq. (11)], and the time scale asso-

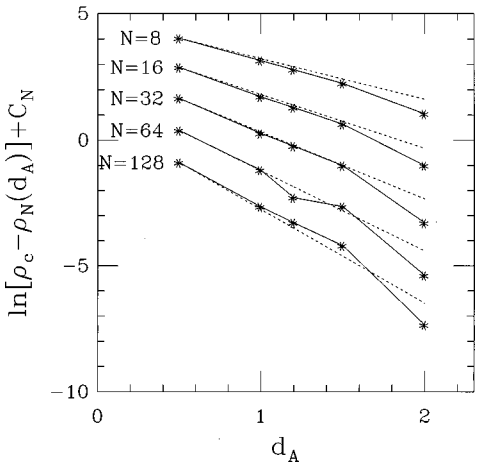

FIG. 8. Open system mean density as a function of driving rate d_A for different system sizes N, offset by constant additive amounts C_N in order to distinguish the results for different N. The dotted lines represent extrapolations of the predicted results based on the hydrodynamic singular diffusion limit from smaller d_A where it is valid, to larger d_A, where the diffusion limit is known to break down. The fact that the solid curves, reflecting the gap (marked by individual data points) between the open system densities and the critical point, fall below the extrapolated values (dotted lines) indicates that the density exceeds the extrapolated value in agreement with our prediction.

ciated with diffusive relaxation τ_D [Eq. (12)]. As we generalize our results to situations in which the transport coefficient exhibits finite size effects, the time scale associated with addition remains the same, while the time scale associated with relaxation will be longer than that given in Eq. (12), because Eq. (12) presumes that events and thus transport are not subject to limitations imposed by the system size. This in turn implies that the density will exceed the value that would have been predicted by the deterministic diffusion limit.

To test this numerically, we note that in the regime where diffusion holds we expect to obtain the scaling given in Eq. (10), where b is given by Eq. (13). For fixed N, the diffusion limit predicts the density will approach the singularity in a manner which scales exponentially with the driving rate d_A:

$$\rho_c-\rho_N\sim\frac{1}{N^{d_A/(\phi-1)}}. \tag{29}$$

However, for d_A sufficiently large, the diffusion limit fails. This in turn implies that for fixed N and large enough d_A Eq. (29) will underestimate the density ρ_N, and the true density is expected to be closer to the singularity. This is consistent with our numerical results, illustrated for the exchange model using full system densities in Fig. 8. For each N when d_A is sufficiently large, the full system density gap ($\rho_c-\rho_N$) systematically drops below the extrapolated scaling law (29), indicative of the fact that the mean density is above the predicted value based on the hydrodynamic diffusion limit. An even sharper drop off is obtained for large d_A when the middle quarter density distributions are used, and similar results are obtained for thermal driving.

Finally, we note that a more detailed fit of $D(\rho)$ would yield an estimate of b for the crossover and saturation regimes. If the saturation value scales like $D(\rho)\sim N^{\theta}$, the time scale associated with relaxation in Eq. (12) which would be replaced by

$$\tau_D\sim N^{2-\theta} \tag{30}$$

in the hard driving regime. Balancing this with the addition rate τ_A yields the modified scaling law describing the rate of approach to the singularity $b=d-d_A+\theta-2$. However, because of the computational resources required to determine the finite size scaling function (27) precisely, we are only able to verify the more conservative prediction of a more rapid approach to ρ_c than would have been expected had the deterministic diffusion limit applied.

VI. CONCLUSION

We have demonstrated a correspondence between a certain class of open SOC models and closed systems which display dynamical phase transitions. In this picture, the open system events distribution is compared to a distribution we construct from an ensemble of closed systems of the same finite size, with a distribution of densities which matches the density fluctuations of the open system, and excluding systems which exceed their sample dependent depinning density. We find that this correspondence always exists independently of how the system is driven and the driving rate. As a byproduct, we have also obtained correlation length exponents on the open system which are consistent with the ones obtained previously on the closed systems, and suggested an extended relationship between closed system relaxation and open system transport which applies to the open SOC models even in the hard driving regime.

Determining whether local equilibrium applies is an important issue in many nonequilibrium systems. Our studies suggest the validity of local equilibrium for the general class of BTW sandpile models, and the result is somewhat surprising given the fact that it persists even when the transitions are long range and the density is fluctuating in the neighborhood of a critical point. However, we expect that these systems may be special. In examples for which the closed, equilibrium system develop site-site correlations, hard driving on the open system is likely to destroy the correlations. The fact that this class of models does not exhibit a diverging site-site correlation length at ρ_c makes it a likely candidate for local equilibrium.

What about systems for which local equilibrium breaks down? In these cases the descriptions of the open and closed systems must be fundamentally different. We already have examples of this kind of behavior in SOC models, including those introduced and studied in Refs. [30,31]. Developing a more systematic understanding of the differences between open and closed systems in these cases remains an important open problem.

ACKNOWLEDGMENTS

This work was supported by the David and Lucile Packard Foundation and NSF Grant Nos. DMR-9212396 and PHY94-07194.

[1] H. Tanaka, Phys. Rev. E **51**, 1313 (1995).
[2] J. Casas-Vazquez and D. Jou, Phys. Rev. E **49**, 1040 (1994).
[3] A. Vespignani and S. Zapperi, Phys. Rev. Lett. **78**, 4793 (1997); **77**, 4560 (1996).
[4] J. Urbach, R. Madison, and J. Markert, Phys. Rev. Lett. **75**, 276 (1995).
[5] J. Krug and P. Ferrari, J. Phys. A **29**, L465 (1996).
[6] D. Fisher, K. Dahmen, S. Ramanathan, and Y. Ben-Zion, Phys. Rev. Lett. **78**, 4885 (1997).
[7] K. Leung, J. Andersen, and D. Sornette, Phys. Rev. Lett. **80**, 1916 (1998).
[8] W. Klein, J. Rundle, and C. Ferguson, Phys. Rev. Lett. **78**, 3793 (1997).
[9] J. Rundle, W. Klein, S. Gross, and D. Turcotte, Phys. Rev. Lett. **75**, 1658 (1995).
[10] P. Bak, C. Tang, and K. Wiesenfeld, Phys. Rev. Lett. **59**, 381 (1987); Phys. Rev. A **38**, 364 (1988).
[11] O. Narayan and D. S. Fisher, Phys. Rev. Lett. **68**, 3615 (1992); Phys. Rev. B **46**, 11 520 (1992).
[12] O. Narayan and A. A. Middleton, Phys. Rev. B **49**, 244 (1994).
[13] J. M. Carlson, J. T. Chayes, E. R. Grannan, and G. H. Swindle, Phys. Rev. Lett. **65**, 2547 (1990).
[14] J. M. Carlson and G. H. Swindle, Proc. Natl. Acad. Sci. USA **92**, 6712 (1995).
[15] J. M. Carlson, E. R. Grannan, G. H. Swindle, and J. Tour, Ann. Prob. **21**, 1372 (1993).
[16] J. M. Carlson, E. R. Grannan, and G. H. Swindle, Stoch. Proc. Appl. **47**, 1 (1993).
[17] J. M. Carlson, E. R. Grannan, and G. H. Swindle, Phys. Rev. E **47**, 93 (1993).
[18] J. M. Carlson, E. R. Grannan, C. Singh, and G. H. Swindle, Phys. Rev. E **48**, 688 (1993).
[19] S. N. Coppersmith and P. B. Littlewood, Phys. Rev. B **36**, 311 (1987).
[20] H. Fukuyama and P. A. Lee, Phys. Rev. B **17**, 535 (1978); P. A. Lee and T. M. Rice, *ibid.* **19**, 3870 (1979).
[21] C. R. Myers and J. P. Sethna, Phys. Rev. B **47**, 11 171 (1993); C. R. Myers, Ph.D. thesis, Cornell University, 1991 (unpublished).
[22] D. S. Fisher, Phys. Rev. Lett. **50**, 1486 (1983); Phys. Rev. B **31**, 1396 (1985).
[23] A. A. Middleton and D. S. Fisher, Phys. Rev. Lett. **66**, 92 (1991); Phys. Rev. B **47**, 3530 (1993).
[24] C. Tang and P. Bak, Phys. Rev. Lett. **60**, 2347 (1988).
[25] J. T. Chayes, L. Chayes, D. S. Fisher, and T. Spencer, Phys. Rev. Lett. **57**, 2999 (1986).
[26] It remains an outstanding problem to explain the quantitative differences between the exponents. See Ref. [27].
[27] A. Montakhab, Ph.D. thesis, University of California, Santa Barbara, 1997 (unpublished).
[28] Our α is equivalent to $1+\kappa/d$ in the notation of Ref. [12].
[29] L. P. Kadanoff, A. B. Chhabra, A. J. Kolan, M. J. Feigenbaum, and I. Procaccia, Phys. Rev. A **45**, 6095 (1992).
[30] L. Kadanoff, S. Nagel, L. Wu, and S. Zhou, Phys. Rev. A **39**, 6524 (1989).
[31] A. A. Middleton and C. Tang, Phys. Rev. Lett. **74**, 742 (1995).